### Title

The thermodynamic response of soft biological tissues to pulsed ultraviolet laser irradiation




### Journal

Biophysical Journal, 69(4)

### ISSN

0006-3495



### Authors

Venugopalan, V
Nishioka, NS
Mikić, BB



### Publication Date

1995-10-01

### DOI

10.1016/s0006-3495(95)80024-x

# The Thermodynamic Response of Soft Biological Tissues to Pulsed Ultraviolet Laser Irradiation

V. Venugopalan,*‡ N. S. Nishioka,* and B. B. Mikić‡
*Wellman Laboratories of Photomedicine, Harvard Medical School, Massachusetts General Hospital, Boston, Massachusetts 02114; and ‡Department of Mechanical Engineering, Massachusetts Institute of Technology, Cambridge, Massachusetts 02139 USA

ABSTRACT The physical mechanisms that enable short pulses of high-intensity ultraviolet laser radiation to remove tissue, in a process known as laser ablation, remain obscure. The thermodynamic response of biological tissue to pulsed laser irradiation was investigated by measuring and subsequently analyzing the stress transients generated by pulsed argon fluorine (ArF, $\lambda$ = 193 nm) and krypton fluorine (KrF, $\lambda$ = 248 nm) excimer laser irradiation of porcine dermis using thin-film piezoelectric transducers. For radiant exposures that do not cause material removal, the stress transients are consistent with rapid thermal expansion of the tissue. At the threshold radiant exposure for ablation, the peak stress amplitude generated by 248 nm irradiation is more than an order of magnitude larger than that produced by 193 nm irradiation. For radiant exposures where material removal is achieved, the temporal structure of the stress transient indicates that the onset of material removal occurs during irradiation. In this regime, the variation of the peak compressive stress with radiant exposure is consistent with laser-induced rapid surface vaporization. For 193 nm irradiation, ionization of the ablated material occurs at even greater radiant exposures and is accompanied by a change in the variation of peak stress with radiant exposure consistent with a plasma-mediated ablation process. These results suggest that absorption of ultraviolet laser radiation by the extracellular matrix of tissue leads to decomposition of tissue on the time scale of the laser pulse. The difference in volumetric energy density at ablation threshold between the two wavelengths indicates that the larger stresses generated by 248 nm irradiation may facilitate the onset of material removal. However, once material removal is achieved, the stress measurements demonstrate that energy not directly responsible for target decomposition contributes to increasing the specific energy of the plume (and plasma, when present), which drives the gas dynamic expansion of ablated material. This provides direct evidence that ultraviolet laser ablation of soft biological tissues is a surface-mediated process and not explosive in nature.

## GLOSSARY

### Nomenclature

| | |
|---|---|
| $A$ | mass number, (−) |
| $c$ | speed of light in vacuum = $2.99792 \times 10^8$ m s$^{-1}$ |
| $c_a$ | propagation speed of a longitudinal acoustic wave (m s$^{-1}$) |
| $c_i$ | propagation speed of a longitudinal acoustic wave in region $i$, $i$ being an integer (m s$^{-1}$) |
| $c_p$ | specific heat at constant pressure (J kg$^{-1}$ K$^{-1}$) |
| $c_v$ | specific heat at constant volume (J kg$^{-1}$ K$^{-1}$) |
| $C$ | capacitance, ($F$) |
| $e$ | proton charge = $1.60219 \times 10^{-19}$ C |
| $e_{33}$ | piezoelectric stress constant of the PVDF film (CN$^{-1}$) |
| $E_\lambda$ | photon energy with wavelength $\lambda$ (eV) |
| exp(x) | exponential of $x$ |
| Fo | Fourier number of laser irradiation relative to the optical penetration depth (= $\alpha\mu_a^2 t_p$), (−) |
| $Fo_\delta$ | Fourier number of laser irradiation relative to the size of a tissue matrix element (= $\alpha t_p/\delta^2$) (−) |
| $\bar{g}$ | Gaunt factor (−) |
| $h$ | specific enthalpy (J kg$^{-1}$) or Planck's constant = $6.62618 \times 10^{-34}$ J s |
| $\hbar$ | $h/2\pi$ = $1.05459 \times 10^{-34}$ J s |
| $k$ | Boltzmann constant = $1.38066 \times 10^{-23}$ J K$^{-1}$ |
| ln(x) | natural logarithm of $x$ |
| $m_e$ | electron mass = $9.10953 \times 10^{-31}$ kg |
| $m_p$ | proton mass = $1.67265 \times 10^{-27}$ kg |
| $\dot{m}''$ | mass flux (kg m$^{-2}$ s$^{-1}$) |
| $M_i$ | Mach number of flow in region $i$, (= $u_i/c_i$), (−) |
| $n_e$ | electron density (m$^{-3}$) |
| $n_i$ | ion density (m$^{-3}$) |
| $n_p$ | proton density (m$^{-3}$) |
| $\mathcal{O}(x)$ | on the order of $x$ |
| $p_i$ | pressure in region $i$, $i$ being an integer (Pa) |
| $q''$ | laser irradiance (W m$^{-2}$) |
| $q_0''$ | incident laser irradiance, (W m$^{-2}$) |
| $R$ | universal gas constant = 8.314 J mol$^{-1}$ K$^{-1}$ |
| $S$ | optical thickness of a plasma layer, (−) |
| $t$ | time, (s) |
| $t_p$ | laser pulse duration, (s) |
| $T$ | temperature, (K) |
| $T_e$ | electron temperature, (K) |
| $T_\infty$ | ambient temperature, (°C) |
| $u_i$ | velocity in region $i$, $i$ being an integer, (m s$^{-1}$) |
| $u_p$ | plasma velocity (m s$^{-1}$) |
| $u_s$ | shock velocity (m s$^{-1}$) |
| $u_v$ | vapor velocity (m s$^{-1}$) |
| $u_i$ | specific volume in region $i$, $i$ being an integer (m$^3$ kg$^{-1}$) |
| $V$ | voltage ($V$) |
| $W$ | work done per unit area (J m$^{-2}$) |
| $x_A$ | mass fraction of component $A$ (−) |
| $z$ | vapor thickness (m) |
| $Z$ | atomic number (−) |

### Greek Symbols

| | |
|---|---|
| $\alpha$ | thermal diffusivity (m$^2$ s$^{-1}$) |
| $\delta$ | characteristic size of the tissue chromophore (m) |
| $\delta_{etch}$ | thickness of tissue etched away by the ablation process (m) |
| $\Delta H$ | change in enthalpy (J mol$^{-1}$) |
| $\Delta S$ | change in entropy (J mol$^{-1}$ K$^{-1}$) |

*Received for publication 6 February 1995 and in final form 5 July 1995.*

Address reprint requests to Vasan Venugopalan, Massachusetts General Hospital, M/S: BHX 630, 50 Blossom St., Boston, MA 02114. Tel.: 617-726-1589; Fax: 617-726-4103; E-mail:vasan@wlp.mgh.harvard.edu.



0006-3495/95/10/1259/13 $2.00

$\epsilon_0$ permittivity of free space = $8.85419 \times 10^{-12}$ C$^2$ J$^{-1}$ m$^{-1}$
$\epsilon$ specific internal energy (J kg$^{-1}$)
$\epsilon_0''$ incident radiant exposure (J m$^{-2}$)
$\epsilon_{th}''$ threshold radiant exposure at which bulk material removal is achieved (J m$^{-2}$)
$\epsilon'''$ volumetric energy density (J m$^{-3}$)
$\epsilon_{th}'''$ threshold volumetric energy density at which bulk material removal is achieved ($= \mu_a \epsilon_{th}''$) (J m$^{-3}$)
$\Phi_i$ $\mathbf{M}_i$ ($\mathbf{M}_i^2 + 3$)/2 (−)
$\gamma_i$ ratio of specific heats ($= c_p/c_v$) in region $i$ (−)
$\lambda$ laser wavelength (m)
$\Lambda$ multiplicative constant used in scaling law for rapid surface vaporization (kg$^{1/3}$m$^{-1}$s$^{-2/3}$)
$\Lambda_{max}$ largest allowable value for $\Lambda$, defined by Eq. 4 (kg$^{1/3}$m$^{-1}$s$^{-2/3}$)
$\Lambda_p$ multiplicative constant used in scaling law for plasma-mediated ablation (kg$^{1/4}$m$^{-1}$s$^{-1/2}$)
$\mu_a$ optical absorption coefficient of incident radiation within target (m$^{-1}$)
$\mu_a^p$ plasma optical absorption coefficient (m$^{-1}$)
$\Omega$ Arrhenius damage integral defined by Eq. 7
$\pi$ 3.14159...
$\Pi$ compression ratio across the shock front produced by rapid surface vaporization, defined by Eq. 16
$\rho$ material density (kg m$^{-3}$)
$\sigma_p$ peak compressive stress (Pa)
$\sigma_{th}$ peak compressive stress generated by irradiation at the threshold radiant exposure $\epsilon_{th}''$ (Pa)
$\tau_m$ dimensionless mechanical equilibration time of the layer heated by laser irradiation ($= \mu_a c_a t_p$), (−)
$\Xi$ defined by Eq. 25, (m$^6$ kg$^{-2}$ s$^{-3}$)

## INTRODUCTION

Pulsed lasers are widely used in surgery because of their ability to rapidly and precisely coagulate, incise, and excise tissue. They are currently employed in numerous applications in a range of surgical subspecialties such as gynecology, ophthalmology, orthopedics, otolaryngology, and neurosurgery (Dixon, 1982). Despite the widespread use of lasers, the physical mechanisms that control laser-tissue interactions are poorly understood. A deeper understanding of these processes would facilitate the development of new laser applications, avoid potential deleterious effects of laser radiation, and advance basic research dealing with biological effects that stem from these interactions. This has motivated many investigators to examine the mechanisms by which pulsed laser radiation removes biological tissue. Over the last decade research has shown that tissue removal, also termed laser ablation, can be mediated by photothermal (e.g., vaporization, pyrolysis), photomechanical (e.g., thermally induced fracture), and perhaps photochemical (e.g., ablative photodecomposition) mechanisms (Albagli et al., 1994a; Srinivasan et al., 1987; Walsh et al., 1988; Zweig, 1991). The relative contribution of these mechanisms to the onset of material removal can be modulated through the appropriate choice of laser wavelength, optical penetration depth, laser spot size and pulse duration. Nevertheless, it is still not possible to make an *a priori* prediction of the mechanism that leads to the onset of material removal when the laser and tissue parameters are specified. Such a capability would be tremendously powerful, since it would lead to a better prediction of the physical and biological response of tissue to a given laser-tissue interaction. In addition, this capability would limit the number of experiments necessary to assess the suitability of a laser and optimize its parameters for a given clinical application.

Such a conceptual understanding of these processes, and the conditions under which they are operative, is more likely to be achieved when a time-resolved measurement of the dynamic response of tissue to irradiation is combined with theoretical analysis to relate the measurements with characteristics of known phenomena. As ablation processes are confined to small spatial and temporal scales, both tasks are difficult because of the limitations of existing experimental approaches and inadequate information about the dynamic optical and physical properties of tissues. In this study we measure the stress transients generated by pulsed ultraviolet (UV) laser irradiation and ablation of tissue and analyze this information to determine the mechanism that mediates the interaction.

In this report, time-resolved stress measurements are combined with modeling and theoretical analysis to characterize the dynamics of pulsed UV laser irradiation and ablation of soft biological tissues. The measurement of laser-induced stress transients was chosen because these stresses arise through transient heating of the target as well as by recoil of ablated material. This permits an examination of the mechanisms responsible for the onset of material removal at very low radiant exposures as well as any changes in the ablation mechanism that may occur at larger radiant exposures once material removal has been achieved. In this respect, the measurement of stress transients has broader applicability than other diagnostic techniques such as flash photography, pump-probe techniques to measure plume dynamics, and interferometric techniques that measure front surface deformation of the target (Albagli et al., 1994a; Domankevitz and Nishioka, 1990; Walsh and Deutsch, 1991). In addition, because the recoil stresses generated by laser ablation of tissues have been shown to cause cellular injury in the region surrounding the ablation site (Doukas et al., 1995; Lustmann et al., 1992; Yashima et al., 1991), the magnitude and temporal structure of the stresses generated by ablative recoil are of great interest. This may facilitate a correlation between the characteristics of the stress transients and the extent of the resulting cellular injury.

Material removal requires the breaking of bonds, which can be achieved by several processes. For example, irradiation causes the rapid thermal expansion of the tissue whose associated mechanical stresses may cause material fracture (Dingus and Scammon, 1991). Alternatively, the absorption of laser energy may produce a phase change in the cellular or extracellular tissue elements or the tissue water. Also, possible modification of the tissue's mechanical integrity through the absorption of radiant energy must be considered. In this study we examine the following two hypotheses.

First, we postulate that the chromophore and its role in preserving the mechanical structure of tissue are important factors that affect the mechanism and dynamics of the

ablation process when the following two conditions are satisfied. 1) The laser pulse duration $t_p$ is small relative to the characteristic thermal diffusion time across the optical penetration depth, $1/\alpha\mu_a^2$. This condition is satisfied when the Fourier number is less than or on the order of 1. That is, when $\mathrm{Fo} = \alpha\mu_a^2 t_p \leq \mathcal{O}(1)$, where $\alpha$ and $\mu_a^{-1}$ are thermal diffusivity of the tissue and the characteristic optical penetration depth of the laser radiation (scattering is assumed negligible), respectively. 2) The laser pulse duration $t_p$ is small relative to the characteristic thermal diffusion time across the characteristic length scale of the chromophore $\delta^2/\alpha$. That is, when $\mathrm{Fo}_\delta = \alpha t_p/\delta^2 \leq \mathcal{O}(1)$, where $\delta$ is the characteristic size of the tissue chromophore.

Under these conditions, energy transport away from the heated volume via diffusion is negligible during irradiation, and the energy absorbed by the chromophore is not transported to neighboring structures. Thus, deposited energy is confined to the tissue chromophore and selective photothermolysis (Anderson and Parrish, 1983) of the chromophore should be considered as a potential mechanism for laser ablation. If the chromophore is the tissue extracellular matrix (ECM), the mechanical integrity of the tissue is directly targeted and may result in the breaking of bonds to allow material removal. Conversely, if the chromophore does not play an active role in preserving the mechanical integrity of tissue, the dynamics of material removal should be quite different. For example, if water is the dominant chromophore (e.g., infrared (IR) laser ablation), the mechanical integrity of the ECM is not targeted directly. In this case, to achieve material removal the heated water must expand, thereby straining and finally fracturing the ECM components. This would likely lead to a slower, albeit more explosive, dynamic process. As such, one may expect a fundamentally different ablation mechanism by simply changing the tissue chromophore without changing parameters which would alter the thermal and mechanical transients that are generated on the macroscopic scale. There is circumstantial evidence to support this hypothesis. A recent study by Edwards et al. (1994) presents results (gross histology and mass removal data) that indicate that ablation of tissue using 6.45 $\mu$m radiation absorbed primarily by the amide II band of the collagen molecule may cause material removal of soft tissues through modification of the tissue collagen. Such a process would be unlike other IR ablation processes where water is the dominant chromophore (Edwards et al., 1994). However, data that would directly point to a different dynamic process in this case are still lacking.

Second, we postulate that the contribution of photomechanical mechanisms to material removal are likely to be significant only when the magnitude of laser-induced stresses is sufficient to cause mechanical fracture or induce cavitation. As suggested by Albagli et al. (1994b), a mechanical mechanism for material removal should be energetically more efficient than vaporization processes because every bond in the ablated mass need not be broken for material fracture. The contribution of photomechanical mechanisms to material removal should become significant when the stresses generated at radiant exposures below the onset of material removal approach the ultimate tensile strength of the target. This is likely to occur when the laser pulse duration $t_p$ becomes shorter or comparable to the mechanical equilibration time of the heated volume. That is, when the dimensionless mechanical equilibration time of the laser-heated layer, $\tau_m = \mu_a c_a t_p \leq \mathcal{O}(1)$ where $c_a$ is the speed of longitudinal wave propagation in the medium.

In this study the stress transients generated in reticular porcine dermis by nanosecond pulses of 193 and 248 nm radiation were measured in vitro. By using ultraviolet wavelengths, the dynamics of ablation in which the tissue ECM is directly targeted by the radiation can be examined. Also, because mechanical equilibration of the heated volume is allowed during 193 nm irradiation and disallowed for 248 nm irradiation, the contribution of photomechanical mechanisms to the material removal process when the tissue ECM is directly targeted is also examined.

At both 193 and 248 nm, collagen is the dominant chromophore of the laser radiation in reticular dermis (Venugopalan, 1994). Collagen type I is the primary ECM protein in the dermis, comprising roughly 30% of the dermis by weight and responsible for maintaining the structural integrity of the dermis (Parry and Craig, 1984). Specifically, 193 nm radiation is likely absorbed by the peptide bonds (—CONH—) along the backbone of the collagen molecule. For 248 nm radiation the aromatic amino acids tryptophan, tyrosine and phenylalanine, present as residues in the primary protein sequence of collagen, are the dominant chromophores. The contribution of nucleic acids, which absorb light about 10 times more strongly as do the aromatic amino acids at 248 nm, can be ignored since the reticular dermis is almost acellular and nearly devoid of nucleic acids (Lynch et al., 1987). Thus, for irradiation at these wavelengths the mechanism for the onset of tissue removal should bear direct connection to the absorption of laser radiation by the collagen within the reticular dermis or by the stress transients induced by the absorption of laser energy.

## MATERIALS AND METHODS

Thin sections of porcine reticular dermis (≈400 $\mu$m thick) were prepared using a pneumatic vibrating dermatome (Zimmer, Concord, MA) from specimens acquired immediately postmortem. Samples were kept refrigerated and hydrated in saline (Baxter Healthcare Corp., Deerfield, IL) until use. Sections were irradiated within 18 hours of acquisition with pulses generated by an excimer laser (Lambda Physik EMG 103/MSC, Acton, MA) using either argon fluorine or krypton fluorine gas fills. The specific laser and tissue parameters and the characteristic time scales involved in the laser-tissue interaction are shown in Table 1.

The active element of the stress transducer was a 9 $\mu$m thick film of piezoelectric polyvinylidene fluoride film with 60 nm thick aluminum electrodes vapor deposited on both sides (AMP Inc., Harrisburg, PA). The sections of dermis were acoustically coupled to the film surface with a thin layer of saline. The film was attached to a plexiglas stub using rubber cement. This stub has an acoustical impedance nearly identical to the tissue and serves as a medium through which stress waves can pass from the tissue. The electrical output of the transducer was taken via a 320 mm long coaxial cable and 50 Ω matching resistor in series to a 1-MΩ impedance preamplifier (Tektronix 7A26, Beaverton, OR) and digitizer (Tektronix

**TABLE 1 Relevant laser parameters and dimensionless time scales for ArF and KrF-excimer laser irradiation of porcine dermis**

| Laser | $\lambda$ (nm) | $E_\lambda$ (eV) | $t_p$ (ns) | $\mu_a^{-1}$ ($\mu$m) | $\tau_m$ ($= \mu_a c_a t_p$) | Fo ($= \alpha\mu_a^2 t_p$) | $Fo_\delta$* ($= \alpha t_p/\delta^2$) |
|---|---|---|---|---|---|---|---|
| KrF-excimer | 248 | 5.0 | 24 | 30‡ | 1.2 | $3.5 \times 10^{-6}$ | $0.3–3.0 \times 10^{-2}$ |
| ArF-excimer | 193 | 6.4 | 22 | 0.35§ | 94 | $3.2 \times 10^{-2}$ | $0.3–3.0 \times 10^{-2}$ |

*A range for this parameter exists because the diameter of collagen fibrils vary between 1 and 3 $\mu$m in reticular dermis (Smith et al., 1982).
‡Value reported by Dyer and Al-Dhahir (1990).
§Value derived by applying a Beer's law model for material blow-off from etch depth versus radiant exposure data as presented by (Ediger et al., 1993). This value represents an upper bound for $\mu_a^{-1}$ because material removal commences during the laser pulse.

AD 7912, 750-MHz bandwidth). In this arrangement, the time-varying voltage $V(t)$ generated between the film electrodes by a uniaxial stress transient whose stress component perpendicular to the film surface $\sigma(t)$ is given by Dyer and Srinivasan (1986) and Schoeffmann et al. (1988):

$$V(t) = \frac{e_{33}}{C_D + C_L} A\sigma(t), \quad (1)$$

where $e_{33}$ is the piezoelectric constant of the PVDF film in pure compression; $C_D$ and $C_L$ are the capacitances of the transducer and the load, respectively; and $A$ is the surface area of the region affected by the stress transient. The temporal resolution of the transducer is $\leq$5 ns (Venugopalan, 1994) and provides a reproducible response for stresses up to $\sigma = 10^{10}$ Pa (Lee et al., 1990). The signal recorded by the digitizer was transferred to a microcomputer (Macintosh LC, Apple Computer, Cupertino, CA) via an RS-232 port.

The optical components were arranged as shown in Fig. 1. An 8-mm diameter aperture was used to select a uniform potion of the laser output. The laser beam then propagated through a set of attenuators, a beam splitter, a 160-mm focal length lens, and a prism that deflected the beam onto the target surface. The optics were composed of UV-grade quartz. The laser pulse energy incident on the target was determined by measuring the energy of the split-off portion of the beam with a pyroelectric detector (Molectron Detector, Inc., Portland, OR, Model J3-09) and correcting for the reflection losses at the optical interfaces and the absorption losses in the quartz optics. The pulse energy was varied by changing the number and/or thickness of quartz flats used as attenuators. The average radiant exposure $\epsilon_0''$ incident on the target surface was calculated by dividing the incident laser energy by the area of the irradiated spot. The spot area was determined by the pattern formed by laser irradiation on laser burn paper (Kentek, Pitsfield, NH) which was found to correspond to the $1/e^2$ spot size within $\pm$20%.

The measurements were made as follows. The tissue sample was placed on the transducer surface with a thin layer of saline in between to provide acoustic contact. The sample was sufficiently thick to absorb all the delivered radiation. The irradiation resulted in the generation of stresses within the heated region as well as recoil stresses imparted to the tissue surface when material removal was achieved. These stresses traversed the tissue thickness and stressed the piezoelectric film, thereby producing the measured voltages. To ensure that the stress waves remained planar during their transit across the tissue thickness, the laser spots used were always >1 mm in diameter. This eliminated geometric attenuation of the stress wave and minimized effects of acoustic absorption and dispersion on the stress transient (Sigrist, 1986; Venugopalan, 1994). The large spot size also ensured that the expansion of ablated material away from the target surface took place in a one-dimensional geometry.

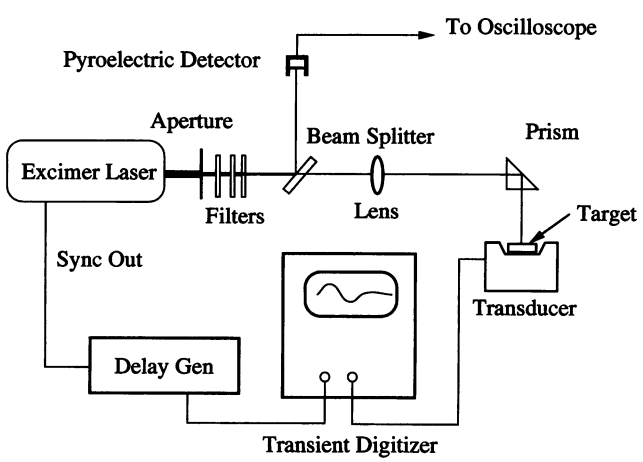


FIGURE 1 Experiment setup for measurement of laser-induced stress transients in tissue.

## RESULTS

### KrF-excimer laser experiments: ($\lambda$ = 248 nm)

Typical signals from the transducer generated by KrF-excimer laser irradiation ($\lambda$ = 248 nm) of porcine dermis are shown in Fig. 2. A positive stress denotes compression and each trace is normalized relative to its peak compressive stress. The signals produced by radiant exposures ranging from a subablative energy dose to a strongly ablative dose are represented by traces 2 a–d. Trace 2 *a* is a bipolar stress transient, (i.e., it has both compressive and tensile components) and is characteristic of stress transients produced by the rapid thermal expansion of the tissue (Dyer and Al-Dhahir, 1990), sometimes referred to as the thermoelas-

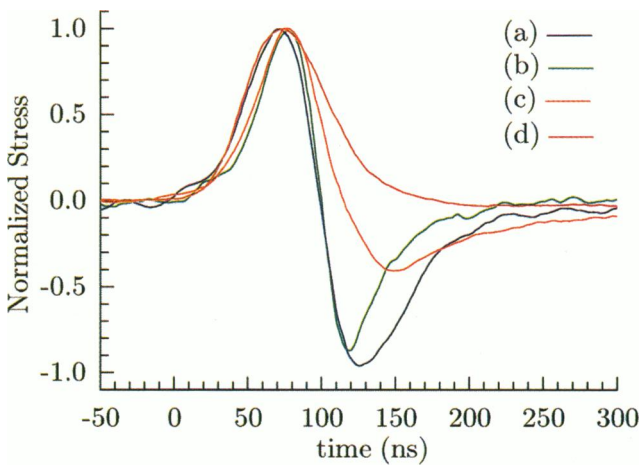


FIGURE 2 Transducer signals resulting from KrF-excimer laser irradiation ($\lambda$ = 248 nm) of porcine dermis in air. The radiant exposure and peak compressive stress for each trace are: (*a*) $\epsilon_0'' = 420$ J m$^{-2}$, $\sigma_p = 5.2 \times 10^6$ Pa; (*b*) $\epsilon_0'' = 2060$ J m$^{-2}$, $\sigma_p = 2.4 \times 10^6$ Pa; (*c*) $\epsilon_0'' = 2200$ J m$^{-2}$, $\sigma_p = 2.6 \times 10^6$ Pa; (*d*) $\epsilon_0'' = 1.1 \times 10^4$ J m$^{-2}$, $\sigma_p = 2.0 \times 10^7$ Pa.

tic effect. The stresses return to baseline in approximately 220 ns. As the radiant exposure is increased to the threshold radiant exposure of ablation (as determined in the Analysis section), the stress transient (*trace* 2 *b*) remains essentially unchanged with the exception that the tensile portion of the thermoelastic stress recovers to baseline more quickly. Once the radiant exposure exceeds this threshold, the magnitude of the tensile portion of the stress wave is reduced relative to the compressive component as shown in trace 2 *c*. Finally, at large radiant exposures where material removal is observed visually, the tensile stresses produced by the thermoelastic mechanism are completely obscured by the compressive recoil stress imparted to the tissue surface by the ablation products. In this case, only a unipolar compressive stress transient is measured. This stress transient reaches its maximum value on the same time scale as the thermoelastic stresses and returns to baseline after a few hundred nanoseconds.

The peak compressive stress $\sigma_p$ generated by KrF-excimer laser irradiation of porcine dermis is plotted versus incident radiant exposure in Fig. 3. For radiant exposures below ablation threshold, the peak stress increases linearly with radiant exposure as expected from thermoelastic stress generation. However, at a radiant exposure $\epsilon_0'' \approx 2000$ J m$^{-2}$ the peak compressive stress produced by ablative recoil dominate those produced by the thermoelastic response and the variation of the peak compressive stress versus incident radiant exposure deviates from this linear behavior.

### ArF-excimer laser experiments: (λ = 193 nm)

Typical stress transients generated by 193 nm (ArF-excimer laser) ablation of porcine dermis are shown in Fig. 4. Each trace is normalized relative to its peak compressive stress.

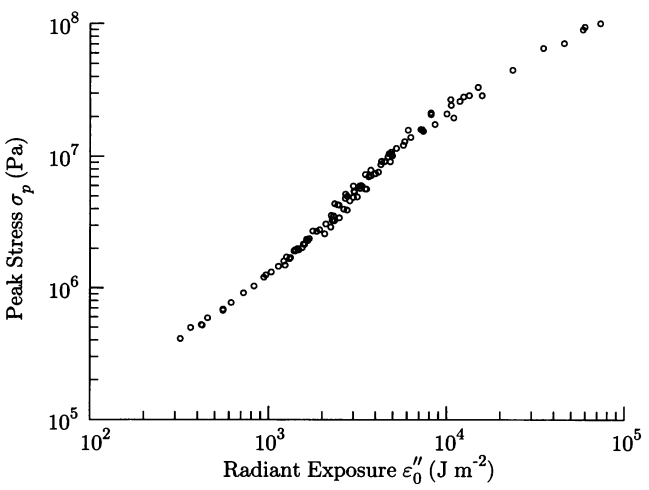


FIGURE 3 Peak compressive stress generated by KrF-excimer laser (λ = 248 nm) irradiation of porcine dermis $\sigma_p$ versus incident radiant exposure $\epsilon_0''$.

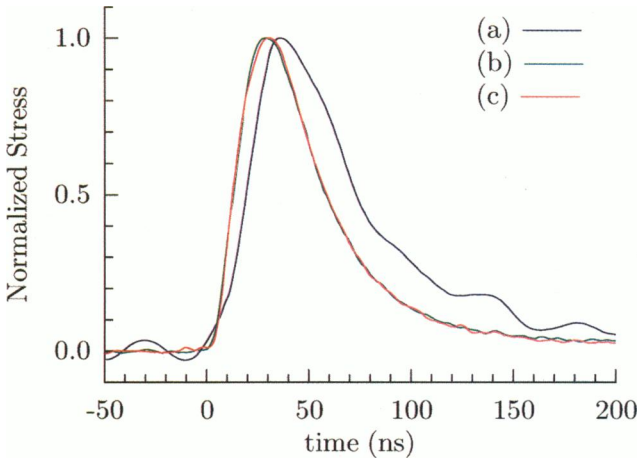


FIGURE 4 Transducer signals generated by ArF-excimer laser ($\lambda$ = 193 nm) of porcine dermis in air. The radiant exposure and peak compressive stress for each trace are: (*a*) $\epsilon_0'' = 570$ J m$^{-2}$, $\sigma_p = 1.1 \times 10^6$, Pa; (*b*) $\epsilon_0'' = 2160$ J m$^{-2}$, $\sigma_p = 1.4 \times 10^7$ Pa; (*c*) $\epsilon_0'' = 5280$ J m$^{-2}$, $\sigma_p = 3.9 \times 10^7$ Pa.

No thermoelastic stresses resulting from 193 nm irradiation were observed. The transients shown in Fig. 4 result from the ablation of porcine dermis by pulsed 193 nm radiation at radiant exposures, the first (Fig. 4, *trace a*) at a radiant exposure close to the ablation threshold, the second and third (Fig. 4, *traces b, c*) at much higher radiant exposures). The transients are purely compressive and remain nearly unchanged with regard to their temporal structure, with the exception that the rise time of the transient decreases slightly with increasing radiant exposure. The peak compressive stress generated by ArF-excimer laser ablation of porcine dermis is plotted versus incident radiant exposure in Fig. 5. For incident radiant exposures larger than $\epsilon_0'' \approx 1200$ J m$^{-2}$ a visible flash was occasionally observed at the time of irradiation over the ablation site and was always observed for $\epsilon_0'' \geq 2500$ J m$^{-2}$.

## ANALYSIS

### KrF-excimer laser irradiation

Three characteristics of the stress transients produced by 248 nm irradiation of porcine dermis require further consideration. First, stress transients consistent with the thermoelastic effect are measured for radiant exposures below the threshold radiant exposure for material removal. The appearance of stress transients whose temporal structure and magnitude are consistent with a thermoelastic response indicates that at subablative exposures, the laser energy, which is absorbed by exciting electronic bands within the collagen molecule, is quickly transferred to the vibrational modes causing heating of the collagen fibrils within the dermis.

Second, as the incident radiant exposure was increased, the tensile component of the waveform became smaller

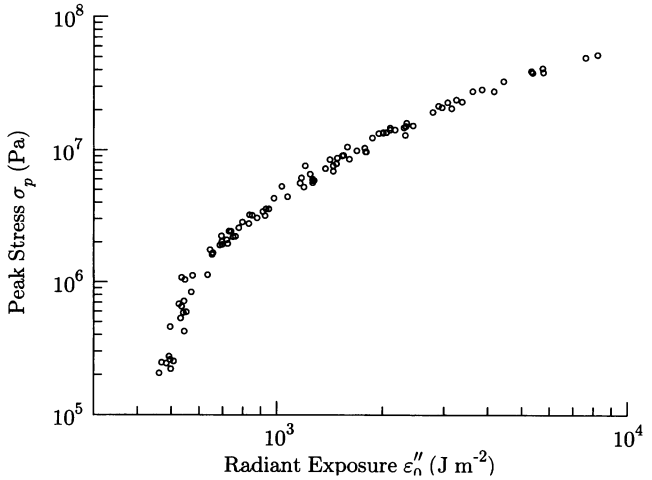


FIGURE 5 Peak compressive stress generated by ArF-excimer laser ($\lambda$ = 193 nm) ablation of porcine dermis $\sigma_p$ versus incident radiant exposure $\epsilon_0''$. Plasma was occasionally observed for $\epsilon_0'' \geq 1200$ J m$^{-2}$ and consistently observed for $\epsilon_0'' \geq 2500$ J m$^{-2}$.

relative to the compressive component and was entirely nonexistent at the highest incident radiant exposures tested. The reduction of the tensile component of the stress wave is likely due to the onset of material removal on the same time scale as the generation of the thermoelastic stresses. The recoil imparted by the ablated material leaving the surface provides a compressive stress, which serves to cancel a portion of the tensile stress generated by the thermoelastic mechanism. At higher radiant exposures the tensile component of the thermoelastic stress is not seen because the compression provided by material removal dominates the tensile component of the thermoelastic stresses. This is also evident in Fig. 3 where the variation of peak stress with incident radiant exposure is no longer linear above $\epsilon_0'' \approx$ 2000 J m$^{-2}$.

Last, over the range of radiant exposures tested, the rise time of the stress transients remains nearly constant. That is, the rise time of the thermoelastic stress transients and stress transients generated by the recoil of ablation products are essentially identical (Fig. 2, *traces a* and *d*). Thus, the onset of material removal for KrF-excimer laser ablation appears to commence during irradiation as has been corroborated by other studies (Cross et al., 1987; Dyer and Al-Dhahir, 1990; Srinivasan et al., 1987).

High-speed photographic studies of tissue ablation using ArF- and KrF-excimer lasers indicate that the plume generated by ArF- and KrF-excimer laser ablation of tissue is composed of fine droplets of condensed material (Puliafito et al., 1987a). This suggested that ablation may be successfully modeled as a rapid surface vaporization process and allow a prediction of the measured stresses once the the process of ablative recoil dominates thermoelastic stress generation. To model this process we assume that surface absorption of the laser energy creates vapor of high temperature and pressure adjacent to the target surface during irradiation. The expansion velocity of the vapor $u_v$ is assumed to be large compared with the sound velocity in the surrounding medium $c_1$. This results in the radiation of a shock wave traveling at velocity $u_s$. Fig. 6 is a schematic of this situation, where the vaporization process is modeled as a piston moving at a velocity $u_v$ into the surrounding gas.

The assumption that a supersonic flow is generated by laser ablation can be rationalized as follows. Applying momentum conservation at the tissue surface, the expansion velocity of the ablated products can be estimated as $u_v \approx \sigma_p t/\rho\delta_{etch}$, where $t$ is the characteristic time over which the material is ejected, $\sigma_p$ is the peak stress, $\rho$ is the tissue density, and $\delta_{etch}$ is the depth to which the tissue has been removed. If we take $t \approx 80$ ns (the width of the ablative stress transient at the half peak stress level) and $\rho = 1000$ kg m$^{-3}$, and we consider 193 nm ablation, at two radiant exposures (e.g., $\epsilon_0'' = 700$ and 5000 J m$^{-2}$) the corresponding etch depths $\delta_{etch}$ are 0.1 and 0.8 $\mu$m, respectively (Ediger et al., 1993). Our measurements give corresponding values for $\sigma_p$ of $2 \times 10^6$ and $3.2 \times 10^7$ Pa, respectively. Substituting these values into the expression above we find $u_v \approx 1600$ and 3200 m s$^{-1}$ at the low and high radiant exposures, respectively. Both values are well in excess of

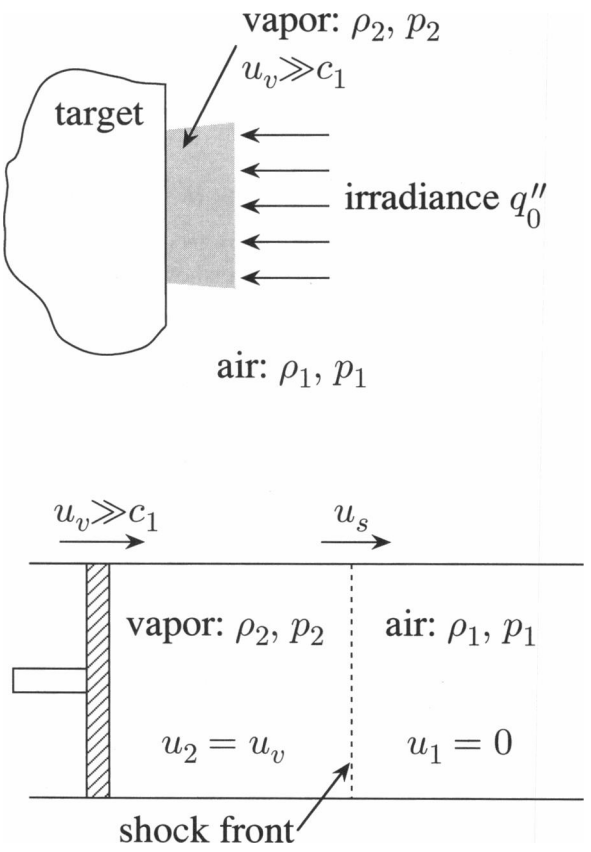


FIGURE 6 Graphic representation of excimer-laser ablation of porcine dermis along with a schematic of the piston model used to describe the process. Velocities in the model representation are given in the laboratory reference frame.

$c_1 = 331$ m s$^{-1}$ under STP conditions, making supersonic flow likely.

Analysis proceeds by solving the mass, momentum, and energy conservation equations to determine the pressure in the vapor $p_2$, which is equal to the recoil stress perpendicular to the target surface. Details of the analysis are presented in Appendix I, and only the result is shown and discussed here. Assuming the velocity of the vapor to be much larger than the speed of sound in the surrounding air $c_1$, the pressure of the vapor adjacent to the target $p_2$ is given by:

$$p_2 = \left\{\left[\frac{\gamma_1(\gamma_1 + 1)p_1}{2}\right]^{1/2} \frac{(\gamma_2 - 1)q_0''}{\gamma_2 c_1}\right\}^{2/3}, \qquad (2)$$

where $p_1$ is the ambient pressure and $\gamma_1$ and $\gamma_2$ are the ratio of specific heats, $c_p/c_v$, in regions 1 and 2, respectively.

Eq. 2 may not be directly applicable to the data because the laser irradiance delivered to the target was not constant in time. Also, because the laser pulses are of such short duration, a steady-state vaporization process may not be established. However, because the dynamics of the ablation process show little temporal delay with respect to the laser pulse (Dyer and Srinivasan, 1986; Srinivasan et al., 1987), changes in the laser irradiance result in a nearly instantaneous change in the ablation dynamics and recoil stress. Thus, we can modify Eq. 2 in the following manner. As the temporal shape of the laser pulse is invariant for changes in $\epsilon_0''$, the incident irradiance $q_0''$ can be replaced by incident radiant exposure divided by the pulse duration, $\epsilon_0''/t_p$. In addition, because the threshold radiant exposure $\epsilon_{th}''$ does not contribute directly to heating the plume of ablated material it should be subtracted from the incident radiant exposure. This leads to the following scaling law for the peak recoil stress:

$$\sigma_p = \Lambda(\epsilon_0'' - \epsilon_{th}'')^{2/3}. \qquad (3)$$

where $\Lambda$ is a parameter that can be adjusted subject to the restriction that it is less than the value given by the steady-state solution, as this would violate the conservation equations. Thus $\Lambda$ must satisfy the condition:

$$\Lambda \leq \Lambda_{max} = \left\{\left[\frac{\gamma_1(\gamma_1 + 1)p_1}{2}\right]^{1/2} \frac{(\gamma_2 - 1)}{\gamma_2 c_1 t_p}\right\}^{2/3}. \qquad (4)$$

The value for $\Lambda_{max}$ is $5.9 \times 10^4$ kg$^{1/3}$ m$^{-1}$ s$^{-2/3}$ for KrF-excimer laser ablation and $6.2 \times 10^4$ kg$^{1/3}$ m$^{-1}$ s$^{-2/3}$ for ArF-excimer laser ablation. A derived value of $\Lambda$ significantly lower than $\Lambda_{max}$ would indicate that a steady-state vaporization process is not achieved early in the laser pulse and that a significant amount of laser energy contributes to the acceleration of the ablated mass to the steady-state velocity.

In Fig. 7 the peak compressive stress data for KrF-excimer laser ablation is shown along with the best fit of scaling law to the data. This fit is achieved with $\Lambda = 5.8 \times 10^4$ kg$^{1/3}$ m$^{-1}$ s$^{-2/3}$ and is nearly identical to but smaller

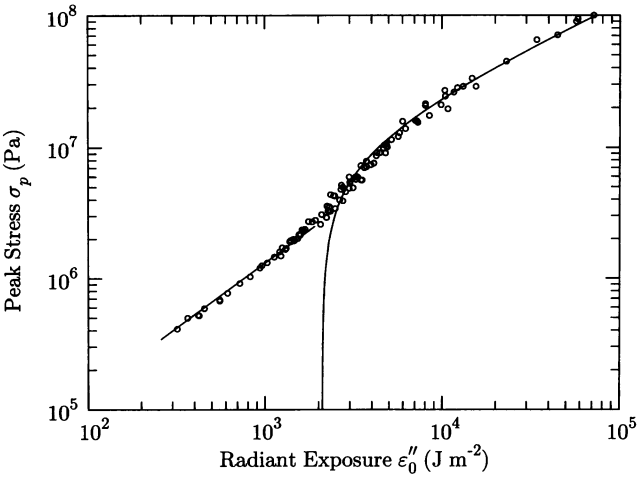


FIGURE 7 Peak compressive stress generated by KrF-excimer laser ($\lambda$ = 248 nm) irradiation of porcine dermis $\sigma_p$ versus incident radiant exposure $\epsilon_0''$. The solid line is the best fit of the thermoelastic data to the scaling $\sigma_p \propto \epsilon_0''$. The solid curve is the best fit of the ablative recoil data to the scaling law for rapid surface vaporization given by $\sigma_p = \Lambda(\epsilon_0'' - \epsilon_{th}'')^{2/3}$ where $\Lambda = 5.8 \times 10^4$ kg$^{1/3}$m$^{-1}$s$^{-2/3}$ and $\epsilon_{th}'' = 2100$ J m$^{-2}$.

than $\Lambda_{max}$. This indicates that the onset of material removal occurs soon after the threshold radiant exposure is delivered and a steady-state vaporization process is established. This is fully consistent with the hypothesis that ablation is achieved through rapid surface vaporization of tissue during irradiation. Note that using this scaling law to fit the data yields a threshold radiant exposure for material removal of $\epsilon_{th}'' = 2100$ J m$^{-2}$, which is much lower than that derived from etch depth studies (Puliafito et al., 1987b) but consistent with other photoacoustic studies (Dyer and Al-Dhahir, 1990). This suggests that the recoil stresses generated by material removal is a more accurate means of determining the threshold radiant exposure for ablation than extrapolations from gross material removal data.

## ArF-excimer laser irradiation

The stresses generated by ArF-excimer laser ablation of porcine dermis differ in many respects from those measured in the KrF-excimer laser irradiation study. No thermoelastic stresses were observed for 193 nm irradiation because the threshold radiant exposure for ablation is smaller, and significant mechanical equilibration of the heated layer occurs during the laser pulse. This results in the generation of thermoelastic stresses smaller than the transducer sensitivity (Venugopalan, 1994). Although thermoelastic stresses were not measured, the stress transients due to ablative recoil have a rise time that indicates that the onset of material removal is rapid and occurs on the time scale of the laser pulse. This is consistent with the results of Srinivasan et al. (1987), who performed similar measurements with $\approx$30 $\mu$m thick samples of bovine cornea and were able to show that

the onset of material removal occurs during irradiation of the target. However, unlike KrF laser irradiation, plasma formation is observed during the ablation process for radiant exposures greater than $\epsilon_0'' \approx 1200$ J m$^{-2}$. This is probably induced by high temperatures within the ablative plume arising from the high volumetric energy density achieved by ArF-excimer laser irradiation. Because the plasma partially absorbs the laser radiation, the gas dynamics of the material removal process is altered and affects the resulting recoil stresses generated by the ablation process.

To model plasma-mediated ablation we consider a one-dimensional geometry and assume the ablation process creates a high-temperature and high-pressure plasma adjacent to the target surface during irradiation. As the plasma expands and cools, it recombines to form a simple vapor. The expansion velocity of the plasma is assumed to be large compared with the sound velocity in the surrounding medium and results in a shock wave traveling at velocity $u_s$. However, because the plasma also absorbs some energy, the shock wave will be followed by a deflagration wave. Fig. 8 is a schematic of this situation along with a representation of the variation in pressure in this flow. Details of this analysis are presented in Appendix II, and only the result is discussed here.

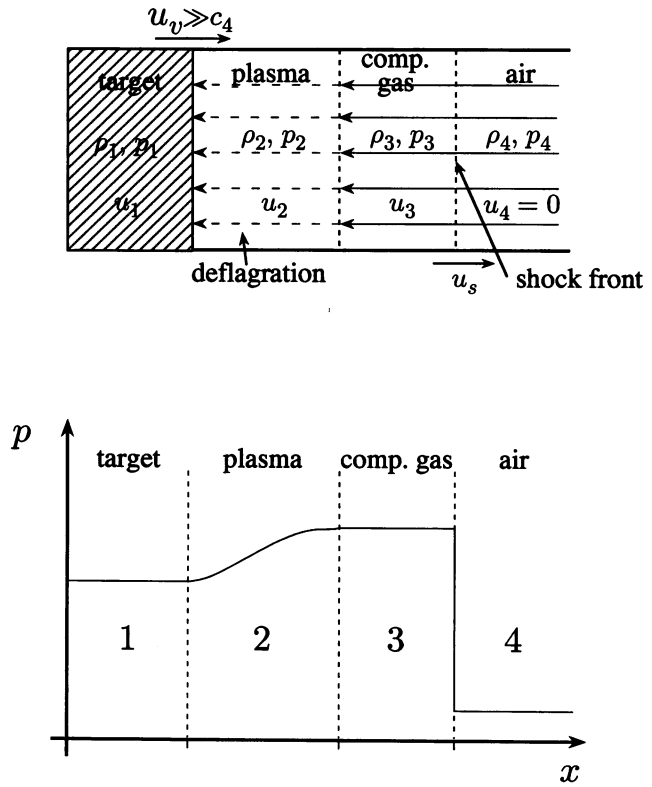


FIGURE 8 Graphic representation of model used to describe the stresses generated by laser-induced plasma formation and expansion.

A gas dynamics analysis yields the following expression for the pressure at the leading edge of the plasma for plasma-mediated ablation processes (Hughes, 1975; Kidder, 1968):

$$p_3 = \left(\frac{S}{\Xi \Phi_3^6}\right)^{1/8} \lambda^{-1/4} t_p^{-1/8} q_0''^{3/4}, \quad (5)$$

where $\lambda$ is the irradiation wavelength, $S$ and $\Xi$ are related to the properties of the plasma, and $\Phi_3$ is related to the dynamics of the ablative flow. $S$, $\Xi$, and $\Phi_3$ can be taken as constant, since they are independent of laser parameters (Kidder, 1968). As in the model for rapid surface vaporization, we cannot use the expression derived from this steady-state analysis directly. Modifying Eq. 5 in the same fashion as we modified Eq. 2 above leads to the following scaling law:

$$\sigma_p = \Lambda_p(\epsilon_0'' - \epsilon_{th}'')^{3/4}, \quad (6)$$

where $\Lambda_p$ is an adjustable parameter for the plasma-mediated ablation.

In Fig. 9 we fit the data to the scaling laws for rapid surface vaporization and plasma-mediated ablation given by Eqs. 3 and 6. Note again that the fit to the rapid surface vaporization data is achieved with $\Lambda = 6.3 \times 10^4$ kg$^{1/3}$ m$^{-1}$ s$^{-2/3}$, which is, as in KrF-excimer laser ablation, practically equal to $\Lambda_{max}$ for ArF-excimer laser ablation. The scaling law for rapid surface vaporization provides an excellent fit to the data at low radiant exposures but underestimates the stresses once the irradiation results in plasma formation. Once plasma formation fully mediates the ablation process, the peak compressive stress is well described by the scaling law for laser-induced plasma formation and expansion. Thus these two models effectively provide lower and upper

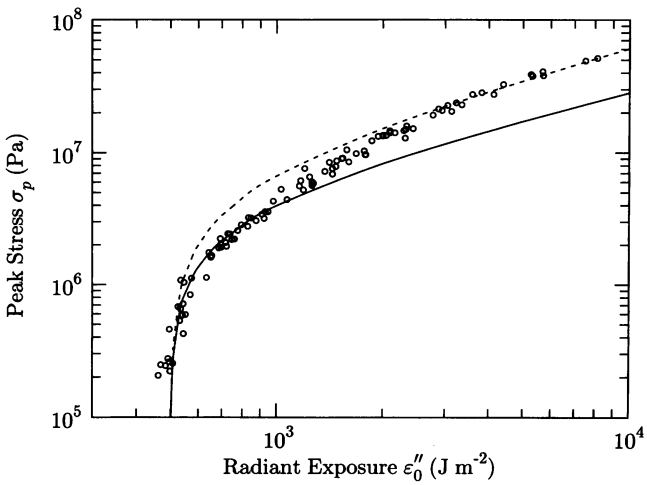


FIGURE 9 Peak compressive stress generated by ArF-excimer laser ($\lambda$ = 193 nm) ablation of porcine dermis $\sigma_p$ versus incident radiant exposure $\epsilon_0''$. (——) Best fit of the ablative recoil data to the scaling law for rapid surface vaporization given by $\sigma_p = \Lambda(\epsilon_0'' - \epsilon_{th}'')^{2/3}$ where $\Lambda = 6.3 \times 10^4$ kg$^{1/3}$m$^{-1}$s$^{-2/3}$ and $\epsilon_{th}'' = 500$ J m$^{-2}$. (----) Best fit of the data to the scaling law for plasma-mediated ablation given by $\sigma_p = \Lambda_p(\epsilon_0'' - \epsilon_{th}'')^{3/4}$ where $\Lambda_p = 6.3 \times 10^4$ kg$^{1/4}$m$^{-1}$s$^{-1/2}$ and $\epsilon_{th}'' = 500$ J m$^{-2}$. Plasma was occasionally observed for $\epsilon_0'' \geq 1200$ J m$^{-2}$ and always observed for $\epsilon_0'' \geq 2500$ J m$^{-2}$.

bounds for the compressive ablative recoil stress generated by 193 nm laser ablation.

## DISCUSSION

For both KrF- and ArF-excimer laser ablation of porcine dermis, we have established that the characteristics of the process are consistent with the view that UV irradiation produces dissolution of the tissue during the laser pulse through the deposition of the threshold incident radiant exposure for ablation $\epsilon''_{th}$. Further, the energy that does not contribute directly to material removal increases the specific energy of the ablation plume, thereby increasing its temperature, which sometimes results in plasma formation and pressure, which drives a gas-dynamic expansion. However, the mechanism by which the vaporization or dissolution of tissue is achieved by the irradiation has not been addressed. While the results of the experiments cannot directly resolve this issue, we can use physical reasoning to infer what these mechanisms might be.

Photomechanical processes are unlikely to be the sole means for material removal because the recoil stresses are consistent with a process of rapid surface vaporization, and the stresses generated at $\epsilon''_{th}$ are much smaller than the ultimate tensile strength (UTS) of porcine dermis, $\sigma_{UTS} \approx$ 8–10 MPa (Yamada, 1970). Accordingly, we search for a mechanism that allows for decomposition or modification of the mechanical integrity of tissue during the laser pulse. This mechanism must provide a direct means for material removal or, in the case of KrF irradiation, allow the substantial thermoelastic stresses generated by the laser irradiation to facilitate material removal. It is possible that temperature rise produced by the absorption of laser energy by the ECM leads to denaturation of tissue proteins on the time scale of the laser pulse (Edwards et al., 1994; Venugopalan, 1994). Because denaturation of collagen is accompanied by the rupture of intermolecular hydrogen bonds (Burdzhanadze and Bezhitadze, 1988), which are necessary for collagen fibers to bear physical stresses (Nimni, 1983), denaturation is a viable mechanism for tissue decomposition.

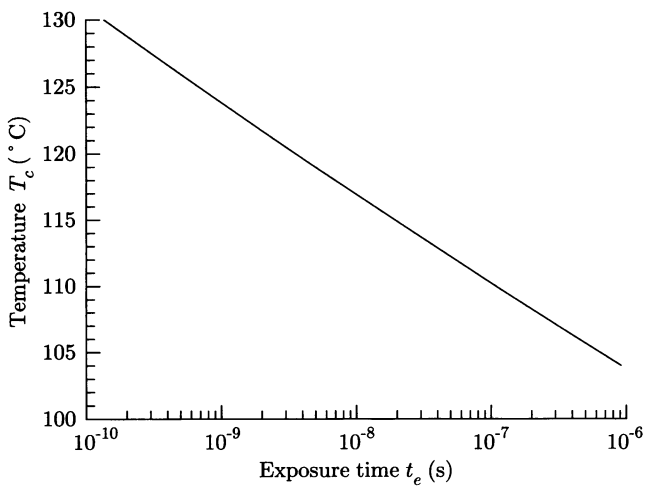


FIGURE 10 Plot of critical temperature, $T_c$ versus exposure time $t_e$ for thermal denaturation of dermis. Denaturation is considered complete when $\Omega = 1$.

To establish the time scale of denaturation, the denaturation process will be treated via the theory of absolute reaction rates. Within this context, denaturation can be thought of as a transformation from a native state $A$ to a denatured state $B$ through a process that passes through an activated state $A^*$, which lies at a Gibbs free energy greater than both states $A$ and $B$. Since the equilibrium concentrations of $A$ and $A^*$ are temperature dependent, the transformation $A \rightarrow B$ is temperature dependent. Thus, to determine the amount of complex $A$ that is converted to $B$, the temperature history must be known. Using the theory of absolute reaction rates one can derive the time-varying concentration of complex $A$ $x_A(t)$ remaining at any time during the temperature transient $T(t)$ (Glasstone et al., 1941):

$$\Omega(t) = -\ln\left[\frac{x_A(t)}{x_A(t=0)}\right] = \int_0^t \frac{kT(t')}{h} \exp\left\{\frac{-[\Delta H - T(t')\Delta S]}{RT(t')}\right\} dt', \quad (7)$$

where $k$, $h$, $\Delta H$, $\Delta S$, and $R$ are the Boltzmann constant, Planck constant, activation enthalpy, activation entropy, and universal gas constant, respectively.

Eq. 7 shows that both enthalpic and entropic contributions are important when considering the kinetics of such rate processes. For protein denaturation both the enthalpy and entropy of activation are quite large (Glasstone et al., 1941). In this limiting case, $\Delta H - T\Delta S$ becomes the difference between two large numbers and the exponential term in Eq. 7 becomes such a strong function of temperature that the preexponential term can be taken as approximately constant. This permits the definition of a critical temperature, $T_c$, such that the region of denaturation (defined as $\Omega = 1$) can be taken as all points where this temperature is reached. This simplification allows $T_c$ to be approximated by the implicit relation (Hu and Barnes, 1970):

$$T_c \approx \frac{\Delta H}{R \ln(kT_c t_e/h) + \Delta S} \quad (8)$$

where $t_e$ is the time the complex is exposed to $T_c$.

For collagen denaturation, the activation enthalpy and entropy have been determined in mouse dermis to be $\Delta H = 4.247 \times 10^5$ J mol$^{-1}$ and $\Delta S = 995.3$ J mol$^{-1}$ K$^{-1}$, respectively (Jacques and Prahl, 1987). This permits a calculation of the critical temperature $T_c$ versus the exposure time, $t_e$. The result of this calculation is shown in Fig. 10, which indicates that a temperature rise of ≈95–100°C is necessary to achieve protein denaturation on a time scale of 1–10 ns

for an initial temperature of 22°C. To determine whether denaturation can be expected to occur over the time scale of the laser pulse, we must find the temperature rise achieved within the ECM of the tissue. If no significant energy losses occur during the irradiation time, the temperature rise in the ECM at the tissue surface is given by:

$$\Delta T = \frac{\mu_a \epsilon_0''}{\rho_{ECM} c_{v,ECM} x_{ECM}}, \quad (9)$$

where $\rho_{ECM}$, $c_{v,ECM}$, and $x_{ECM}$ are the density, specific heat, and mass fraction of the ECM, respectively. Assuming that the properties of the ECM are dominated by the properties of native collagen at a hydration level of 0.35 g $H_2O$/g tissue, $\rho_{ECM}$, $c_{v,ECM}$, and $x_{ECM}$ take values of approximately 780 kg $m^{-3}$, 2300 J $kg^{-1}$ $K^{-1}$, and 0.3, respectively (Long et al., 1993; Mrevlishvili, 1977; Nomura et al., 1977; Parry and Craig, 1984). Thus, KrF-excimer laser irradiation at the threshold radiant exposure of $\epsilon_{th}'' = 2100$ J $m^{-2}$ produces a temperature change at the surface of 130°C that is sufficient to achieve denaturation of tissue during the irradiation. We should also mention that because these experiments were done on a multiple shot basis, the collagen lining the margins of the ablation crater are already denatured. Thus, at low radiant exposures, the laser pulses may be simply removing tissue already denatured by previous pulses. However, at larger radiant exposures, the etch depth is larger than the zone of residual damage, and tissue removal includes material not denatured by previous laser pulses.

The mechanism for material removal in ArF-excimer laser ablation is likely similar to that of KrF-excimer laser ablation. This is manifest in the fact that the scaling law for rapid surface vaporization provides an adequate fit to the ablative recoil stress data before the onset of plasma formation. However, the volumetric energy density necessary for material removal $\epsilon_{th}'''$ is about 20 times larger in the case of ArF-excimer laser ablation. While this discrepancy can be attributed in part to the uncertainty regarding the optical penetration depth of 193 nm laser radiation in tissue (Ediger et al., 1993; Puliafito et al., 1985) it is also likely that the thermoelastic stresses generated by KrF-excimer laser irradiation reduce the energy needed to "detach" the ablated material from the bulk tissue. Because the magnitude of thermoelastic stresses generated at the ablation threshold ($\sigma_{th}$) by 193 nm laser radiation is at least 10 times smaller ($\sigma_{th} = 0.2$ MPa, whereas $\sigma_{th} = 3$ MPa for 248 nm irradiation), they may not facilitate the material removal process which results in the higher energy density necessary to achieve ablation.

This mechanism of material removal achieved through targeted destruction of the tissue chromophore implies that essentially all collagen that is denatured is removed. This may be the key reason why the morphology of in vitro ArF- and KrF- excimer laser etching of tissue is free of gross mechanical injury and exhibits minimal thermal injury (Lane et al., 1985; Puliafito et al., 1985, 1987b). In contrast, with IR ablation using sources such as Q-switched Er:YAG and TEA $CO_2$ lasers, which are absorbed by water, gross mechanical tearing and extensive thermal injury occur (Cummings and Walsh, 1993; Walsh et al., 1988, 1989) despite comparable optical absorption depths. At these wavelengths the material removal process is presumably governed by explosive vaporization of tissue water, which may lead to significant amounts of the thermal energy at the ablation site and induce considerable tissue tearing. However, detailed measurement of the dynamics of the IR laser ablation process will be needed to validate this hypothesis.

## CONCLUSIONS

The stress transients generated by pulsed excimer laser irradiation and ablation of porcine dermis at $\lambda = 193$ and 248 nm have been measured. Modeling and theoretical analysis permits the correlation of the temporal structure and amplitude of the measured transients with the nature and dynamics of the tissue response to UV laser irradiation. Specifically, we have shown that laser exposures that do not achieve material removal produce stress transients that are consistent with dynamic thermal expansion of the tissue known as thermoelastic stress generation. When ablation is achieved the recoil stresses produced at both wavelengths are fully consistent with the view that the onset of material removal occurs during irradiation and proceeds via a process of laser-induced rapid surface vaporization. This permits the formulation of a scaling law that relates the measured recoil stress with the incident and threshold radiant exposures. For 193 nm irradiation, ignition of the ablation plume occurs at high radiant exposures leading to a plasma-mediated ablation process. Again, a gas dynamic analysis permits the formulation of a scaling law that describes the functional variation of the recoil stress with incident radiant exposure in this regime. The success of the rapid surface vaporization and plasma models in predicting the ablative recoil stresses suggests that the ablation process is surface-mediated because energy in excess of that necessary to remove material contributes to the specific energy of the plume and drives the gas dynamic expansion of the ablated debris.

Using the classical theory of absolute reaction rates, we determined that the temperature rise produced by absorption of the threshold radiant exposure by collagen within the tissue ECM can result in its denaturation during irradiation. Since denatured collagen is unable to bear physical stresses, this is a viable mechanism for material removal. The comparison of 193 and 248 nm ablation provides insight into the role of laser-induced stresses with regard to the onset of material removal. At the threshold radiant exposure for ablation, the peak stress amplitude generated by 248 nm irradiation is more than an order of magnitude greater than that produced by 193 nm irradiation. These measurements indicate that the stresses generated by KrF-excimer laser irradiation at the threshold for material removal, while unable to fracture the tissue alone, may facilitate the material

removal process. This may explain why the incident volumetric energy density $\epsilon'''_0$ required to achieve material removal is 20 times higher at 193 nm irradiation than at 248 nm irradiation. Thus, the measurements are consistent with the hypothesis that UV laser ablation is a surface-mediated process that is brought about by the decomposition of the collagen through thermal denaturation.

## APPENDIX

### I. Stresses generated by rapid surface vaporization

As shown for ArF- and KrF-laser irradiation of tissue, the deposition of large volumetric energy densities into a tissue can result in material removal. The experimental results indicate that the characteristics of the material removal bear strong resemblance to a process of rapid surface vaporization. The recoil of the vapor leaving the tissue surface generates a compressive stress pulse that propagates into the tissue bulk. In this appendix, we derive an analytic expression for the recoil stress magnitude generated by a steady process of rapid surface vaporization.

The process of steady vaporization has been considered by many investigators in connection with laser drilling of metals (Afanas'ev and Krokhin, 1967; Anisimov, 1968; Knight, 1979). To derive a scaling law for the recoil stress at the target surface, we will take an approach suggested by Landau and Lifshitz (1987). We consider in one dimension the expansion of a layer of a high temperature and pressure gas created by laser vaporization of the target. The expansion velocity of the vapor $u_v$ is assumed larger compared than the ambient sound velocity $c_1$. This results in the radiation of a shock traveling at velocity $u_s$. Fig. 6 is a schematic of this situation where the vaporization process is modeled as a piston moving at velocity $u_v$ into the surrounding gas. In this case the equations of mass, momentum, and energy conservation in a reference frame moving with the shock wave are:

$$\frac{u_1}{v_1} = \frac{u_2}{v_2} = -\dot{m}'', \tag{10}$$

$$p_1 + \frac{u_1^2}{v_1} = p_2 + \frac{u_2^2}{v_2} \tag{11}$$

and

$$h_1 + \frac{u_1^2}{2} = h_2 + \frac{u_2^2}{2}. \tag{12}$$

In Eqs. 10 and 11, the subscripts 1 and 2 refer to the regions downstream and upstream of the shock wave as indicated in Fig. 6. Thus, region 1 consists of surrounding gas under ambient conditions, and region 2 consists of a mixture of ablation vapor and ambient gas that has undergone shock compression. $h$, $m''$, $p$, $u$, and $v$ refer to specific enthalpy, mass flux per unit area, pressure, velocity, and specific volume, respectively. Combining Eqs. 10 and 11 gives an expression for the velocity of the vapor flow leaving the target surface $u_v$:

$$u_v = u_2 - u_1 = [(p_2 - p_1)(v_1 - v_2)]^{1/2}. \tag{13}$$

Our goal is to express the vapor flow velocity, $u_v$, in terms of the pre- and post-shock pressures, $p_1$ and $p_2$. This is done by combining Eqs. 10–12 and using the relation $h = pv\,[\gamma/(\gamma - 1)]$, where $\gamma$ is the ratio of specific heats ($c_p/c_v$), to get a relation for the ratio of specific volumes across the shock front in terms of the pre- and post-shock pressures:

$$\frac{v_2}{v_1} = \frac{p_1(\gamma_1 + 1) + p_2(\gamma_1 - 1)}{p_1(\gamma_1 - 1) + p_2(\gamma_1 + 1)}. \tag{14}$$

Combining Eqs. 13 and 14 we get the following quadratic equation for the compression ratio, $\Pi = (p_2/p_1)$ across the shock:

$$\Pi^2 - \left[2 + \frac{u_v^2\gamma_1(\gamma_1 + 1)}{2c_1^2}\right]\Pi + \left[1 - \frac{u_v^2\gamma_1(\gamma_1 - 1)}{2c_1^2}\right] = 0, \tag{15}$$

where $c_1 = \sqrt{\gamma_1 p_1 v_1}$ is the adiabatic sound speed in region 1. Solving Eq. 15 for $\Pi$ yields:

$$\Pi = \left[1 + \frac{\gamma_1(\gamma_1 + 1)u_v^2}{4c_1^2}\right] \pm \frac{\gamma_1 u_v}{c_1}\left[1 + \frac{(\gamma_1 + 1)^2 u_v^2}{16c_1^2}\right]^{1/2}. \tag{16}$$

As the velocities of the ablated particles are likely to be supersonic (Puliafito et al., 1987a), we examine Eq. 16 in the limit where the velocity of the vapor is much larger than the speed of sound in the surrounding air, i.e., $u_v \gg c_1$. In this limit, the ratio of pressures across the shock front becomes:

$$\Pi = \frac{\gamma_1(\gamma_1 + 1)u_v^2}{2c_1^2}. \tag{17}$$

To determine $u_v$, conservation of energy is applied globally to the process. When performing this energy balance we assume that the energy necessary to form the vapor and any energy losses to the target are small compared with both the energy that heats the vapor and the work done by the expanding vapor on the surrounding air. In this case, energy conservation can be written as:

$$\frac{d\epsilon}{dt} + \frac{dW}{dt} = q_0'', \tag{18}$$

where $W$ is the work done by the expanding vapor on the surrounding air per unit surface area and $\epsilon$ is the internal energy of the expanding vapor per unit surface area. Letting $z$ denote the thickness of the vapor layer, $W = p_2 dz$ and $\epsilon = p_2 z/(\gamma_2 - 1)$. Substituting these expressions into Eq. 18 (recognizing that $u_v = (dz/dt)$) and substituting Eq. 17 for $p_2/p_1$ yields:

$$u_v = \left[\frac{2(\gamma_2 - 1)c_1^2 q_0''}{\gamma_2\gamma_1(\gamma_1 + 1)p_1}\right]^{1/3}. \tag{19}$$

Substituting Eq. 19 into Eq. 17 and solving for $p_2$ gives:

$$p_2 = \left\{\left[\frac{\gamma_1(\gamma_1 + 1)p_1}{2}\right]^{1/2}\frac{(\gamma_2 - 1)q_0''}{\gamma_2 c_i}\right\}^{2/3}. \tag{20}$$

This is identical to the result shown earlier as Eq. 2.

### II. Stresses generated by plasma formation and expansion

At very high energy densities, the laser irradiation may be sufficient not only to ablate the tissue but also to ionize the ablation products and form a dense plasma adjacent to the target surface. Because the plasma absorbs a significant portion of the incident laser radiation the gas dynamics of the ablative flow is altered substantially. Thus the expression to predict the ablative recoil stress derived in the previous appendix does not apply when plasma mediates the laser-target interaction.

In modeling this situation the velocity of the ablation products is assumed to be much larger than the sound velocity in the ambient gas, thereby radiating a shock wave. However, because a portion of the laser energy is absorbed by the plasma, the shock wave is followed by a

deflagration wave (Kidder, 1968). This collective structure of a shock wave followed by a deflagration wave is called a ZND detonation after Y. B. Zeldovich, J. von Neumann, and W. Döring for their work in analytically describing the internal structure of detonation waves in the 1940s and 1950s (Zucrow and Hoffman, 1976). Fig. 8 is a pictorial representation of the physical situation we are considering along with the spatial variation of pressure within this flow structure. ZND detonation waves fall into the general class of combustion waves. Combustion waves differ from shock waves in that a release of energy occurs within the wave front. In this case, the release of energy is due to absorption of the laser radiation by the plasma. Thus, to model this ablative flow, we must first characterize the absorption of the laser radiation by the plasma.

We consider the case where free-free absorption or inverse Bremsstrahlung is the mechanism responsible for plasma heating. This occurs when an electron absorbs a photon that moves it from one free state to a more energetic state in the field of an ion. Assuming that the plasma collectively has no net charge, its absorption coefficient $\mu_a^p$ in the limit where the photon energy is much less than the electron energy in the plasma (i.e., $h\nu \ll kT_e$) is given by Hughes (1975):

$$\mu_a^p = \frac{2}{3}\sqrt{\frac{\pi}{6}}\,\bar{g}\left(\frac{1}{m_e kT_e}\right)^{3/2}\frac{n_i^2 Z^3 e^6 \lambda^2}{n_p \epsilon_0^3 c^3}, \tag{21}$$

where $\pi$, $\bar{g}$, $m_e$, $T_e$, $n_i$, $Z$, $e$, $\lambda$, $n_p$, $\epsilon_0$, and $c$ are 3.14159, the Gaunt factor, electron mass, electron temperature, ion density, atomic number, electron charge, irradiation wavelength, proton density, permittivity in vacuum, and speed of light, respectively. The specific volume and sound speed in the plasma, $v_2$ and $c_2$, are given by:

$$v_2 = \frac{Z}{Am_p n_e} \tag{22}$$

and

$$c_2 = \left[\frac{(Z+1)\gamma_2 kT_2}{Am_p}\right]^{1/2}. \tag{23}$$

These equations permit the expression of the plasma absorption coefficient in terms of the wavelength of irradiation and hydrodynamic variables:

$$\mu_a^p = \frac{\Xi\lambda^2}{v_2^2 c_2^3}, \tag{24}$$

where

$$\Xi = \frac{2}{3}\sqrt{\frac{\pi}{6}}\,\bar{g}\,\frac{Z^3(Z+1)^{3/2}\gamma^{3/2}e^6}{n_p A^{7/2} m_p^{7/2} m_e^{3/2}\epsilon_0^3 c^3}. \tag{25}$$

We assume that the Chapman-Jouget condition is satisfied and the plasma expands at the speed of sound. This provides the following upper bound on the optical thickness of the plasma $S$:

$$S = \mu_a^p c_3 t_p. \tag{26}$$

We assume that the optical thickness $S = \mathcal{O}(1)$ because if the plasma is transparent (i.e., $S < \mathcal{O}(1)$), the heating rate of the plasma will be small and will lead to an increase in both the rate of target vaporization and optical thickness of the plasma. Conversely, if the plasma is optically thick ($S > \mathcal{O}(1)$), the target will be shielded by the plasma and will lead to a decrease in both the rate of vaporization and the optical thickness of the plasma. Thus, there exists an "equilibrium" optical thickness of the plasma where the rate of expansion of the plasma is compensated by the supply of ionized ablation products through vaporization. Such a situation is referred to as the "self-matched regime" after Krokhin (1965). For our irradiation parameters, this regime is reached in a time small compared with the laser pulse duration (Phipps et al., 1988). Next, we need to determine the relation between the velocity of the plasma expansion and the laser irradiance $q_0''$. We assume that a negligible amount of energy is necessary for vaporization and ionization of the target and that the ablation products are sufficiently characterized as an ideal gas. Applying energy conservation on a control volume that starts at the front surface of the target and encompasses the plasma and the deflagration wave yields the following (Kidder, 1968):

$$\rho_3 u_3 (h_3 + u_3^2/2) = q_0''. \tag{27}$$

Recalling that for an ideal gas $c_a = \sqrt{\gamma pv}$, $h = c_a^3/(\gamma - 1)$ and taking $\gamma = 5/3$ we have

$$q_0'' = \frac{c_3^3}{v_3}\left[\frac{\mathbf{M}_3}{2}(\mathbf{M}_3^2 + 3)\right], \tag{28}$$

where $\mathbf{M}_3$ is the Mach number $= u_3/c_3$. Solving for $v_3$ and $c_3$ from Eqs. 24, 26, and 28 we get the expressions:

$$v_3 = \left(\frac{\Phi_3^{2/3}\Xi}{S}\right)^{3/8}\lambda^{3/4} t_p^{3/8} q_0''^{-1/4} \tag{29}$$

and

$$c_3 = \left(\frac{\Xi}{\Phi_3^2 S}\right)^{1/8}\lambda^{1/4} t_p^{1/8} q_0''^{1/4}, \tag{30}$$

where $\Phi_3 = \mathbf{M}_3(\mathbf{M}_3^2 + 3)/2$. Thus the pressure developed at the leading edge of the plasma due to laser heating is given by the scaling law:

$$p_3 = \frac{c_3^2}{v_3} = \left(\frac{S}{\Phi_3^6 \Xi}\right)^{1/8}\lambda^{-1/4} t_p^{-1/8} q_0''^{3/4}, \tag{31}$$

which is identical to the result presented earlier as Eq. 5. Note that this expression scales with the peak stress at the target surface $\sigma_p$ because the pressure ratio across the deflagration ($p_1/p_3$) is independent of the laser parameters (Kidder, 1968) and can be taken as constant. This result shows that although the plasma mediates the interaction, the dependence of the recoil stress on the optical thickness is very weak. Thus the assumption that the optical thickness be $\mathcal{O}(1)$ is not critical to the final result. Also we find that the recoil stress is weakly dependent on the irradiation wavelength and the laser pulse duration.

We thank the Whitaker Foundation for support of this work through a Biomedical Engineering research grant. We are also grateful to the reviewers for their insightful comments in connection with this manuscript.

## REFERENCES

Afanas'ev, Y. V., and O. N. Krokhin. 1967. Vaporization of matter exposed to laser emission. *Sov. Phys. JETP.* 25:639–645.

Albagli, D., B. Banish, M. Dark, G. S. Janes, C. von Rosenberg, L. T. Perelman, I. Itzkan, and M. S. Feld. 1994a. Interferometric surface monitoring of biological tissue to study inertially confined ablation. *Lasers Surg. Med.* 14:374–385.

Albagli, D., L. T. Perelman, G. S. Janes, C. von Rosenberg, I. Itzkan, and M. S. Feld. 1994b. Inertially confined ablation of biological tissue. *Lasers Life Sci.* 6:55–68.

Anderson, R. R., and J. A. Parrish. 1983. Selective photothermolysis: precise microsurgery by selective absorption of pulsed radiation. *Science.* 220:524–527.

Anisimov, S. I. 1968. Vaporization of metal absorbing laser radiation. *Sov. Phys. JETP.* 27:182–183.

Burdzhanadze, T. V., and M. O. Bezhitadze. 1988. Thermodynamic and structural characterization of partially denatured collagen. *Biofizika.* 33:220–225.

Cross, F. W., R. K. Al-Dhahir, P. E. Dyer, and A. J. MacRobert. 1987. Time-resolved photoacoustic studies of vascular tissue ablation at three laser wavelengths. *Appl. Phys. Lett.* 50:1019–1021.

Cummings, J. P., and J. T. Walsh Jr. 1993. Tissue tearing caused by pulsed laser-induced ablation pressure. *Appl. Opt.* 32:494–503.

Dingus, R. S., and R. J. Scammon. 1991. Grüneisen-stress induced ablation of biological tissue. *Proc. SPIE.* 1427:45–54.

Dixon, J. A. 1982. Surgical applications of lasers. *Proc. IEEE.* 70: 579–588.

Domankevitz, Y., and N. S. Nishioka. 1990. Measurement of laser ablation threshold with a high-speed framing camera. *IEEE J. Quantum Elec.* 26:2276–2278.

Doukas, A. G., D. J. McAuliffe, S. Lee, V. Venugopalan, and T. J. Flotte. 1995. Physical factors involved in stress-wave-induced cell injury: the effect of stress gradient. *Ultrasound Med. Biol.* In press.

Dyer, P. E., and R. K. Al-Dhahir. 1990. Transient photoacoustic studies of laser tissue ablation. *Proc. SPIE.* 1202:46–60.

Dyer, P. E., and R. Srinivasan. 1986. Nanosecond photoacoustic studies on ultraviolet laser ablation of organic polymers. *Appl. Phys. Lett.* 48: 445–447.

Ediger, M. N., G. H. Pettit, R. P. Weiblinger, and C. H. Chen. 1993. Transmission of corneal collagen during ArF excimer laser ablation. *Lasers Surg. Med.* 13:204–210.

Edwards, G., R. Logan, M. Copeland, L. Reinisch, J. Davidson, B. Johnson, R. Maciunas, M. Mendenhall, R. Ossoff, J. Tribble, J. Werkhaven, and D. O'Day. 1994. Tissue ablation by a free-electron laser tuned to the amide II band. *Nature.* 371:416–419.

Glasstone, S., K. J. Laidler, and H. Eyring. 1941. The Theory of Rate Processes. McGraw Hill Book Co. Inc., New York.

Hu, C-L., and F. S. Barnes. 1970. The thermal-chemical damage in biological material under laser irradiation. *IEEE Trans. Biomed. Eng.* BME-17:220–229.

Hughes, T. P. 1975. Plasmas and Laser Light. Adam Hilger Ltd, London.

Jacques, S. L., and S. A. Prahl. 1987. Modeling optical and thermal distributions in tissue during laser irradiation. *Lasers Surg. Med.* 6:494–503.

Kidder, R. E. 1968. Application of lasers to the production of high-temperature and high-pressure plasma. *Nucl. Fusion.* 8:3–12.

Knight, C. J. 1979. Theoretical modeling of rapid surface vaporization with back pressure. *AIAA Journal.* 17:519–523.

Krokhin, O. N. 1965. "Matched" plasma heating mode using laser radiation. *Sov. Phys. Tech. Phys.* 9:1024–1026.

Landau, L. D., and E. M. Lifshitz. 1987. *Fluid Mechanics,* 2nd ed. Pergamon Press, Oxford.

Lane, R. J., R. Linsker, J. J. Wynne, A. Torres, and R. G. Geronemus. 1985. Ultraviolet-laser ablation of skin. *Arch. Dermatol.* 121:609–617.

Lee, L. M., D. A. Hyndman, R. P. Reed, and F. Bauer. 1990. PVDF applications in shock measurements. *In* Shock Waves in Condensed Matter—1989. S. C. Schmidt, J. N. Johnson, L. W. Davison, editors. Elsevier Science Publishers B. V., Amsterdam. 821–824.

Long, C. G., E. Braswell, D. Zhu, J. Apigo, J. Baum, and B. Brodsky. 1993. Characterization of collagen-like peptides containing interruptions in the repeating Gly-X-Y sequence. *Biochemistry.* 32:11688–11695.

Lustmann, J., M. Ulmansky, A. Fuxbrunner, and A. Lewis. 1992. Photoacoustic injury and bone healing following 193nm excimer laser ablation. *Lasers Surg. Med.* 12:390–396.

Lynch, S. E., J. C. Nixon, R. B. Colvin, and H. N. Antoniades. 1987. Role of platelet-derived growth factor in would healing: synergistic effects with other growth factors. *Proc. Natl. Acad. Sci. USA.* 84:7696–7700.

Mrevlishvili, G. M. 1977. Thermodynamic properties of biopolymers in the helical and coiled state in the temperature interval 4–400°K. *Biofizika.* 22:180–191.

Nimni, M. E. 1983. Collagen: Structure, function, and metabolism in normal and fibrotic tissues. *Semin. Arthritis Rheum.* 13:1–86.

Nomura, S., A. Hiltner, J. B. Lando, and E. Baer. 1977. Interaction of water with native collagen. *Biopolymers.* 16:231–246.

Parry, D. A. D., and A. S. Craig. 1984. Growth and development of collagen fibrils in connective tissue. *In* Ultrastructure of the Connective Tissue Matrix. A. Ruggeri and P. M. Motta, editors. Martinus Nijhoff Publishers, Boston, MA. 34–64.

Phipps, Jr., C. R., T. P. Turner, R. F. Harrison, G. W. York, W. Z. Osborne, G. K. Anderson, X. F. Corlis, L. C. Haynes, H. S. Steele, K. C. Spicochi, and T. R. King. 1988. Impulse coupling to targets in vacuum by KrF, HF, and $CO_2$ single-pulse lasers. *J. Appl. Phys.* 64:1083–1096.

Puliafito, C. A., R. F. Steinert, T. F. Deutsch, F. Hillenkamp, E. J. Dehm, and C. M. Adler. 1985. Excimer laser ablation of the cornea and lens. *Ophthalmology.* 92:741–748.

Puliafito, C. A., D. Stern, R. R. Kreuger, and E. R. Mandel. 1987a. High-speed photography of excimer laser ablation of the cornea. *Arch. Ophthalmol.* 105:1255–1259.

Puliafito, C. A., K. Wong, and R. F. Steinert. 1987b. Quantitative and ultrastructural studies of excimer laser ablation of the cornea at 193 and 248 nanometers. *Lasers Surg. Med.* 7:155–159.

Schoeffmann, H., H. Schmidt-Kloiber, and E. Reichel. 1988. Time-resolved investigations of laser-induced shock waves in water by use of polyvinylidenefluoride hydrophones. *J. Appl. Phys.* 63:46–51.

Sigrist, M. W. 1986. Laser generation of acoustic waves in liquids and gases. *J. Appl. Phys.* 60:R83–R121.

Smith, L. T., K. A. Holbrook, and P. H. Byers. 1982. Structure of the dermal matrix during development and in the adult. *J. Invest. Dermatol.* 79:93s–104s.

Srinivasan, R., P. E. Dyer, and B. Braren. 1987. Far-ultraviolet laser ablation of the cornea: photoacoustic studies. *Lasers Surg. Med.* 6:514–519.

Venugopalan, V. 1994. The thermodynamic response of polymers and biological tissues to pulsed laser irradiation. Sc.D. thesis, Massachusetts Institute of Technology, Cambridge, MA.

Walsh, Jr., J. T., and T. F. Deutsch. 1991. Measurement of Er:YAG laser ablation plume dynamics. *Appl. Phys. B.* 52:217–224.

Walsh, J. T. Jr., T. J. Flotte, R. R. Anderson, and T. F. Deutsch. 1988. Pulsed $CO_2$ laser tissue ablation: effect of tissue type and pulse duration on thermal damage. *Lasers Surg. Med.* 8:108–118.

Walsh, J. T. Jr., T. J. Flotte, and T. F. Deutsch. 1989. Er:YAG laser ablation of tissue: effect of pulse duration and tissue type on thermal damage. *Lasers Surg. Med.* 9:314–326.

Yamada, H. 1970. Strength of Biological Materials. Williams & Wilkins, Baltimore, MD.

Yashima, Y., D. J. McAuliffe, S. L. Jacques, and T. J. Flotte. 1991. Laser-induced photoacoustic injury of skin: effect of inertial confinement. *Lasers Surg. Med.* 11:62–68.

Zucrow, M. J., and J. D. Hoffman. 1976. Gas Dynamics. John Wiley and Sons, Inc., New York.

Zweig, A. D. 1991. A thermo-mechanical model for laser ablation. *J. Appl. Phys.* 70:1684–1691.